 doi:10.20944/preprints201909.0185.v1

Article

Removal of Copper Ions in Wastewater by Adsorption onto a Green Adsorbent from Winemaking Wastes

Lorena Alcaraz [1], Irena García-Díaz [1], Francisco J. Alguacil [1] and Félix A. López [1,*]

[1] National Center for Metallurgical Research (CENIM). Spanish National Research Council (CSIC). Avda. Gregorio del Amo, 8. 28040 Madrid, Spain; alcaraz@cenim.csic.es (L.A.); irenegd@cenim.csic.es (I.G.-D.); fjalgua@cenim.csic.es (F.J.A.); f.lopez@cenim.csic.es (F.A.L.)

* Correspondence: f.lopez@cenim.csic.es (F.A.L.)

Abstract: This article presents the copper ions adsorption process using an activated carbon from winemaking wastes. The pH, temperature, activated carbon amount and initial copper concentration were varied based on a full factorial 2^k experimental design. Kinetic and thermodynamic studies were also carried out. The adsorption kinetics was found follow a pseudo-second-order model. The adsorption data fit better to the Langmuir isotherm. The ANOVA demonstrated that both pH of the solution and activated carbon dosage had the greatest influence on copper adsorption. The activation energy was -32 kJ·mol^{-1} suggesting that the copper adsorption is a physic-sorption process. The best fit to a linear correlation was the moving boundary equation that controls the kinetics for the adsorption copper ions onto the activated carbon. The X-ray photoelectron spectroscopy (XPS) results reveal the existence of different copper species (Cu^{2+}, Cu^{+} and or Cu^{0}) on the surface of the carbonaceous adsorbent after the adsorption, which could suggest a simultaneous reduction process.

Keywords: activated carbon; adsorption; copper; winemaking wastes.

1. Introduction

The contamination of water by toxic heavy metals is a worldwide environmental problem that has increasingly focused the attention of the scientific community [1]. Heavy metals such as Cu, Cd, Pb and Zn, among others, are present in the water through the discharge of industrial wastewater and are toxic to human beings and other living species when their concentrations exceed certain values [2]. In humans, the poisoning by copper ingestion may show systemic effects such as hemolysis or liver and kidney damage. In addition, other local effects have been reported such as irritation of upper respiratory tract, gastrointestinal disturbance with vomiting and diarrhea and a form of contact dermatitis [1]. All of these effects contribute to a necessary treatment of the wastewater that containing copper [3]. The U.S. Environmental Protection Agency (EPA) has set a guidance level for copper in drinking water at 1.3 mg·L^{-1} [4].

Copper ions may be present in waters through several sources such as mining operations, machinery, electric power, chemical industry, electroplating processes, petroleum refining or pesticides industries [5]. To copper removal, different methods have been studied such as precipitation [6], on exchange [7], membrane filtration [8] or ionic flocculation [9]. Nevertheless, these remove methods are usually expensive being the adsorption process a highly effective and economical method [3]. Therefore, the adsorption method to remove heavy metal ions from aqueous solutions by a low-cost adsorbent (which is defined as a material that is abundant in nature, or is a by-product or waste material from industry) is a constant research development [2].

Preprints (www.preprints.org) | NOT PEER-REVIEWED | Posted: 17 September 2019 doi:10.20944/preprints201909.0185.v1

In this sense, activated carbons are known as very effective adsorbents. This type of the materials is characterized by have highly porosity, great surface area, variable characteristics of surface chemistry, and high degree of surface reactivity [10,11]. However, active carbons have high production costs and are usually more expensive than other types of adsorbents. For this reason, nowadays, the production of activated carbons from renewable and cheaper precursors have led a growing attention to the researchers [12,13].

In recent years, activated carbons from different wastes such as barley straw [14], pistachio wood [15], coconut shells [16], wild olive cores [17] or winewastes [18] have been tested as effective candidates to carried out metal removal by the adsorption method.

This research describes the obtaining and characterization of activated carbon from a winemaking waste, bagasse. Different experiments were assessed modified the pH value, copper concentration, adsorbent dosage and temperature in order to investigate the adsorbent capacity of copper ions onto AC.

The results were analyzed by a statistical experimental design and the influence of three factors were considered: pH of the solution, metal concentration and adsorbent dosage.

2. Results and discussion

2.1. Adsorption experiment

2.1.1. Influence of the pH of the solution

The pH is a variable that have a great effect on the adsorption process [19]. To evaluate the surface charge of the AC the zeta potential measurements were assessed. The value of PZC for the obtained activated carbon is 3.4. The AC surface is positively charged between 0 to the PZC pH. For pH values higher than 3.4, the AC surface exhibit a negative charge.

The effect of the pH on the Cu adsorption was studied by different experiments. The experimental conditions were 25 mg of activated carbon was added to 100 mL solution containing 0.01 $g \cdot L^{-1}$ of copper ions. The pH of the solutions was adjusted at 1, 3 and 5 using 0.1 M HCl. Figure 1 exhibits the adsorbed copper amount onto the activated carbon versus the contact time.

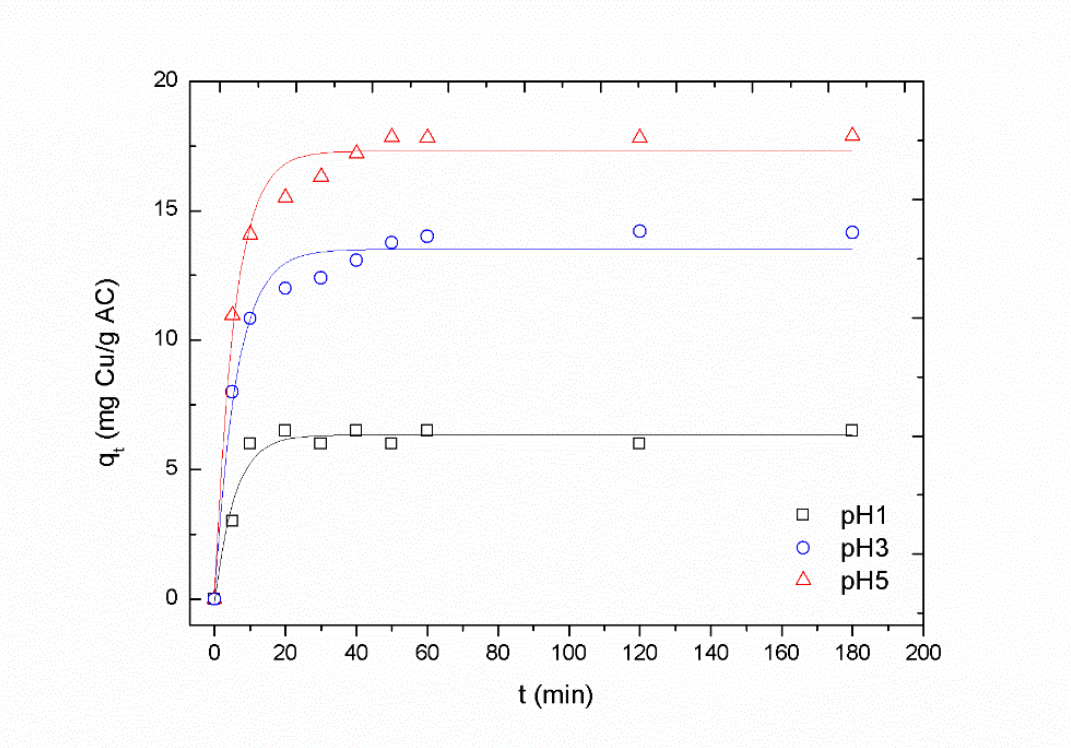

Figure 1. Copper uptake onto the carbon at different pH values as a function of the contact time

Preprints (www.preprints.org) | NOT PEER-REVIEWED | Posted: 17 September 2019 doi:10.20944/preprints201909.0185.v1

The adsorption capacity increases with the solution pH. The Cu^{2+} removal is quite low at pH 1 and 3, this could be due that at these pH values, the surface of the AC is positively charged, so there is electrostatic repulsion between the surface and the metal charge. When the pH increasing pH beyond PZC (i.e., pH 5 value experiment), the negative charge on the AC surface increases, leading to an enhancing the metal adsorption [20]. Thereby, the subsequently experiments were carried out at the pH value where the observed adsorption was maximum.

2.1.2. Effect of Cu^{2+} concentration

The adsorption of different copper concentration (0.005-0.02 $g \cdot L^{-1}$) with an amount of 25 mg of the activated carbon at pH 5 were analyzed (Figure 2). As expected, the removed Cu^{2+} amount decrease with the increase of the initial concentration. However, even in the highest concentration studied, the copper adsorption is nearly to 36 mg Cu/g AC, probably due to the fact of the rapid saturation of the activated sites with a certain metal concentration [21].

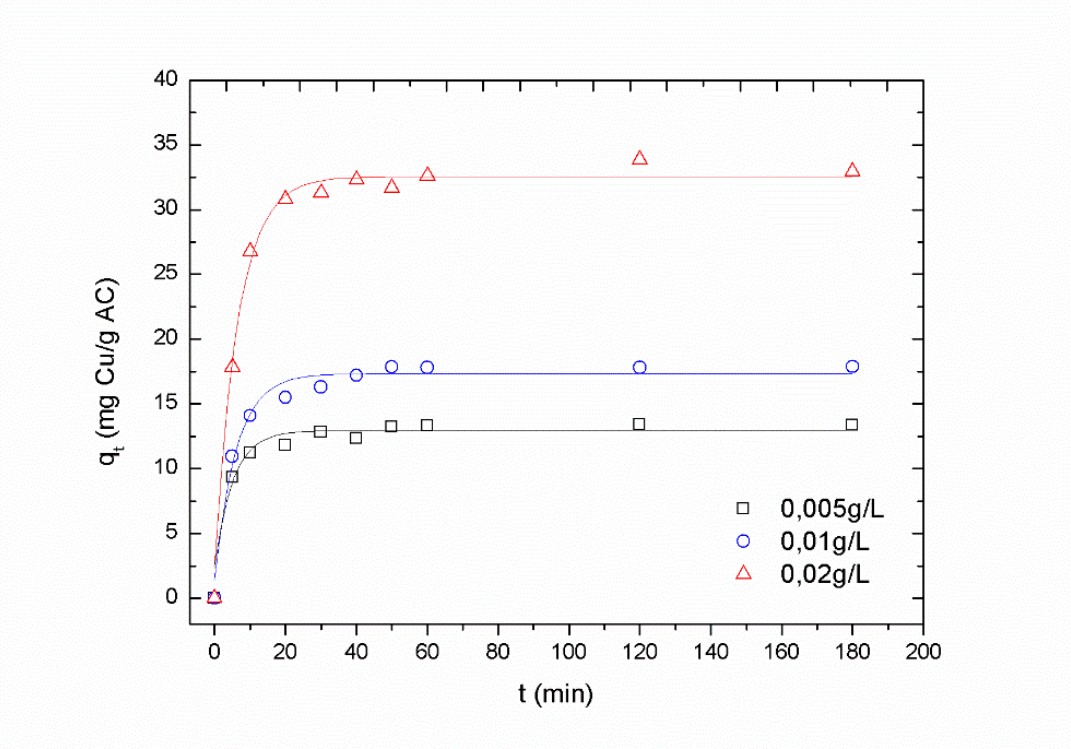

Figure 2. Effect of copper concentration as a function of the contact time.

2.1.3. Effect of activated carbon dosage

In order to evaluate the effect of the adsorbent dosage for Cu^{2+} adsorption, solutions of 0.01$g \cdot L^{-1}$ Cu^{2+} were put in contact with different masses (12.5-75 mg) of the activated carbon at pH 5. Figure 3 shows the obtained results. As can be appreciated the Cu amount adsorbed onto the AC increase with the adsorbent dosage.

Preprints (www.preprints.org) | NOT PEER-REVIEWED | Posted: 17 September 2019 doi:10.20944/preprints201909.0185.v1

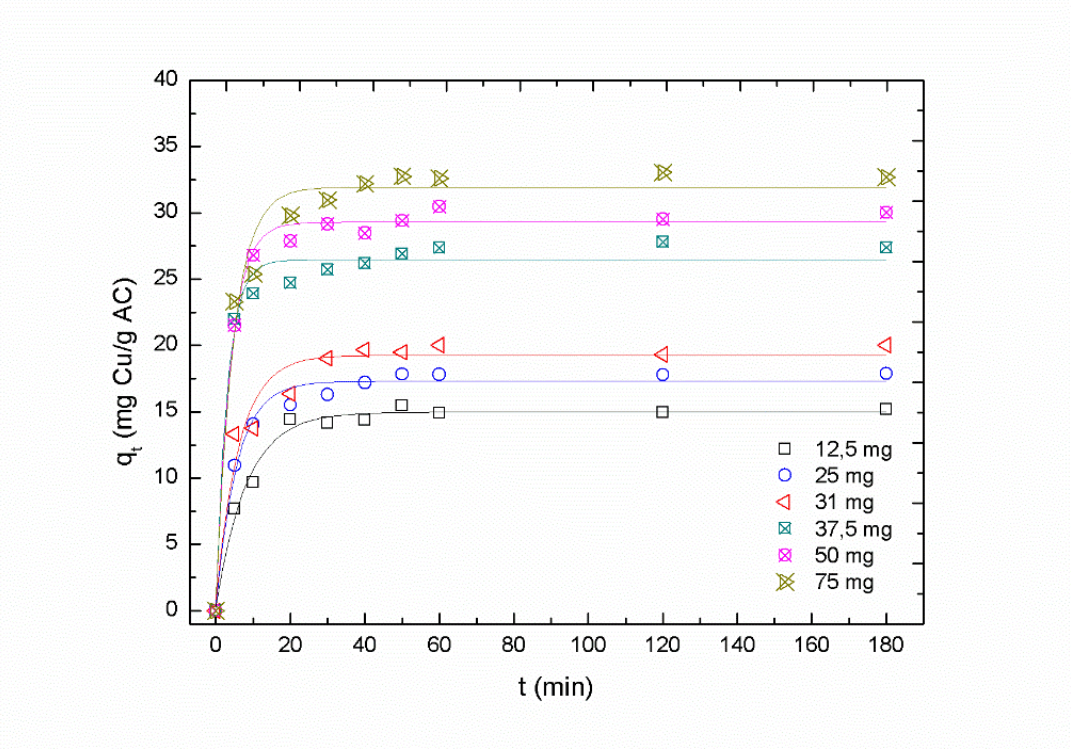

Figure 3. Effect of the adsorbent dosage on metal uptake.

2.1.4. Effect of the temperature

The copper adsorption was analyzed at different temperatures. Figure 4 exhibits copper uptake as a function of time for the different temperatures studied. The amount of copper adsorbed increases when so did the temperature.

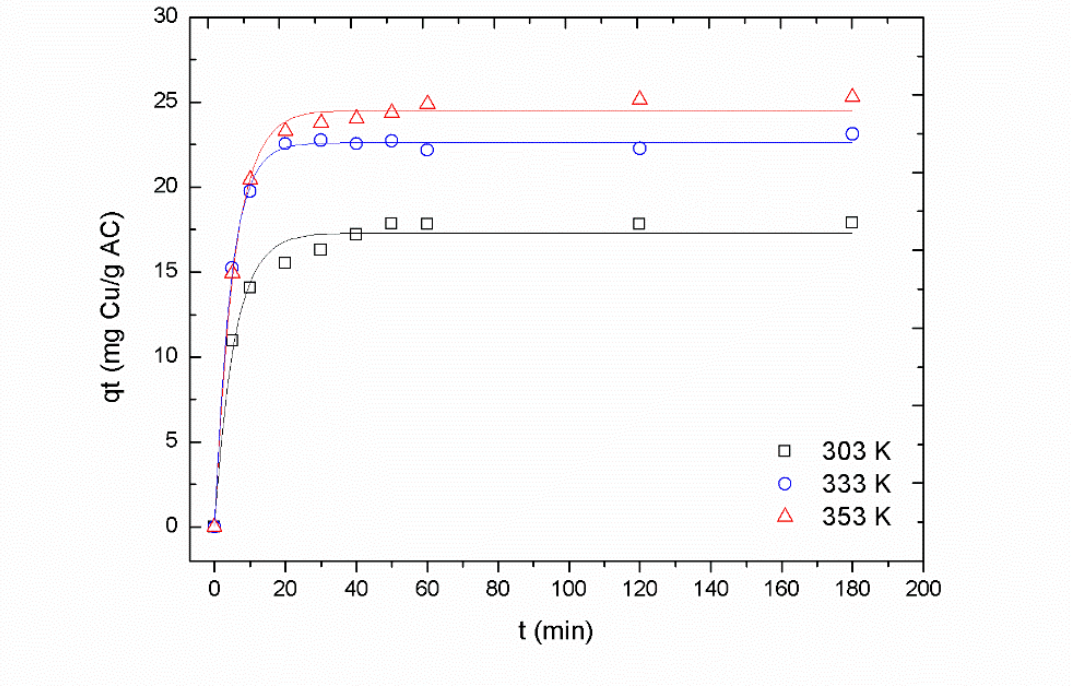

Figure 4. Copper uptake at different temperatures.

Preprints (www.preprints.org) | NOT PEER-REVIEWED | Posted: 17 September 2019 doi:10.20944/preprints201909.0185.v1

2.1.5. Equilibrium isotherms

The study of equilibrium isotherms was carried out using the Langmuir, Freundlich and Temkin equations. The calculated constant parameters and correlation coefficients are given in Table 1.

Table 1. Calculated parameters values for the different linear models.

Langmuir				Freundlich			Temkin		
q_m (mg·g^{-1})	b (L·mg^{-1})	R_L	R^2	K_F (L·g^{-1})	1/n	R^2	A_T	b_T	R^2
16.95	3.94	0.03	0.998	5.91	0.92	0.967	0.82	104.92	0.981

The greater correlation coefficient was obtained for Langmuir isotherm. The maximum adsorption capacity (q_m) calculated from this model is similar to the experimental one 22 mg·g^{-1}. In addition, the Langmuir non-dimensional factor (separation factor, R_L) of 0.03 indicates a favorable adsorption process [4,22].

2.1.6. Kinetic study

The results derived from Figure 4 were used to fit various kinetics models and, the calculated results from these fits are summarized in Table 2.

In all cases, pseudo-second-order model showed significantly higher correlation coefficients than the pseudo-first-order model. The calculated q_e values are in good agreement with the obtained experimental q_e values. In addition, K_2 constant decreased with temperature which indicates that the metal adsorption to occur easily at high temperatures.

Table 2. Kinetic parameters for copper adsorption at different temperatures.

Pseudo-first-order				Pseudo-second-order			
T (K)	R^2	K_1 (min^{-1})	q_e (mg·g^{-1})	R^2	k_2 (g·mg^{-1}·min^{-1})	$q_{e,calc}$ (mg·g^{-1})	$q_{e,exp}$ (mg·g^{-1})
303	0.687	0.04	9.200	0.994	0.131	16.521	17.30
333	0.567	0.07	10.344	0.997	0.048	22.727	22.62
353	0.702	0.05	10.568	0.999	0.020	23.613	24.53

In order to estimate the adsorption type, the kinetics rate constants (ln $k_{2,obs}$) were fitted versus 1/T, with slope $-E_a/R$ [23]. The activation energy is frequently used for differentiating between physical and chemical adsorption. In the case of the physical adsorption, the reactions are readily reversible, equilibrium attained rapidly and thus energy requirements are small (between the range of 5 to 40 kJ·mol^{-1}). However, the chemical adsorption is specific, involves stronger forces and thus requires larger activation energies (40 to 800 kJ·mol^{-1}) [23]. In the present case, the calculated activation was -32 kJ·mol^{-1} which suggested a physic-sorption process.

Table 3 summarized the obtained results of the thermodynamic parameters. The calculated values for enthalpy change (-13.9 kJ·mol^{-1}) and free energy change (-16.53, -32.10 and -33.19 kJ·mol^{-1}) indicate that the copper adsorption by the activated carbon is an exothermic, spontaneous and favorable process.

Preprints (www.preprints.org) | NOT PEER-REVIEWED | Posted: 17 September 2019 doi:10.20944/preprints201909.0185.v1

Table 3. Thermodynamic parameters at different temperatures.

T (K)	$-\Delta H^0$(kJ·mol^{-1})	ΔS^0 (J·mol^{-1}·K^{-1})	$-\Delta G^0$ (kJ·mol^{-1})
303	13.93	54.55	16.53
333			32.10
353			33.19

2.2. Characterization of the AC and AC-Cu

2.2.1. Scanning electron microscopy (SEM)

SEM micrographs of the initial AC and AC-Cu are exhibit in Figure 5. A clear change can be appreciated when the copper is adsorbed onto the AC surface. Initially, a porous structure was observed characteristic of an active carbon. After the Cu adsorption, the pores structure changes where a different contrast was appreciated. In addition, microanalysis carried out which indicates the presence of peak at 1 keV characteristics of Cu k_α in the sample.

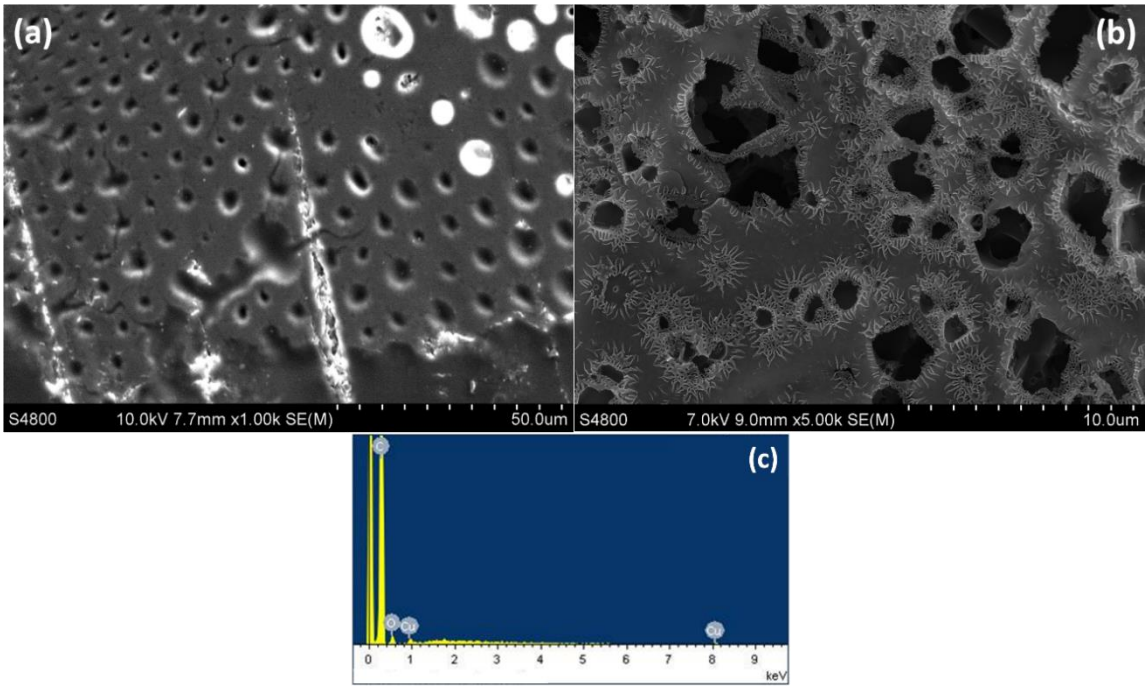

Figure 5. SEM images of the AC (a) before and (b) after the Cu adsorption and (c) EDS microanalysis of the AC-Cu sample.

2.2.2. X-ray photoelectron spectroscopy (XPS) analysis

XPS spectrum of C 1s regions for both AC and AC-Cu samples are depicted in Figure 6a and b. Registered spectra are similar in terms of the shape and position of the bands. A broad and asymmetric band is observed in both cases suggested the existence of different carbon species. The

 doi:10.20944/preprints201909.0185.v1

deconvolution of the bands exhibited four peaks around 285 (C-C bond), 286 (C-OH bond), 288 (C=O bond), and 290 (COOH bond) [24–26].

On the other hand, XPS spectrum for AC-Cu sample concerning Cu 2p core level excitation is shown in Figure 6c in order to understand the electronic structure of copper species at superficial level. The obtained spectrum shows two main peaks centered at around 933 eV and 953 eV which can be attributed with Cu $2p^{3/2}$ and $2p^{1/2}$, respectively. In addition, Cu $2p^{3/2}$ peak exhibits a shoulder band that could be indicating that the Cu^{2+} components are different in chemical environment [27,28] as a previously reported. These observed peaks appeared at ~934.3 eV and ~932.6 eV and can be assigned to octa-coordinated of Cu^{2+} ions and tetra-coordinated of Cu^{+}-Cu^{0} species [27,28]. It should be noted it is difficult to distinguish between Cu^{+} and Cu^{0} peaks, since the Cu 2p binding energies of both species are very close [29]. So, the obtained results suggested that Cu^{2+} could be reduced to Cu^{+} even Cu^{0}. Despite of the kinetic studies shown that the adsorption process is a physic-sorption process, the obtained results from XPS analyses could be suggest a chemisorption process. Finally, the band at 945 eV can be assigned at satellite bands. This band is generated by an electron transfer from a ligand orbital to a 3d orbital of Cu. Therefore, since Cu^{0} or Cu^{+} species have completely filled d level, the observed satellite band confirms that the Cu^{2+} specie are present in the surface of the material [28,30,31].

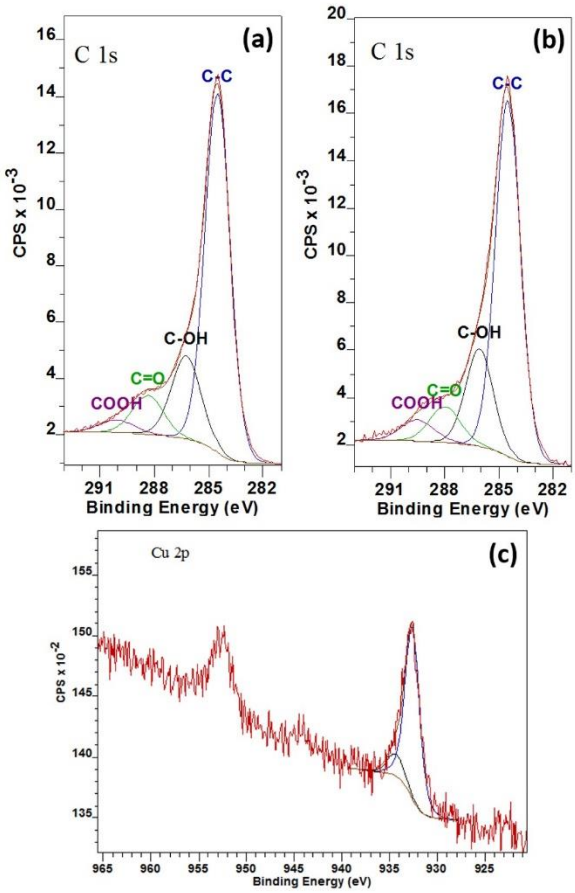

Figure 6. XPS spectra of the activated carbon and AC-Cu activated carbon.

2.3. Post-treatment of the adsorption process

2.3.1. Scanning electron microscopy (SEM)

To investigate about the possibilities to recover copper from the Cu(II)-bearing solutions, and as a first approach, these were precipitated with sodium borohydride. As a result of this precipitation a near black solid is yielded, which apparently is formed by cuprite and zero valent copper.

Preprints (www.preprints.org) | NOT PEER-REVIEWED | Posted: 17 September 2019 doi:10.20944/preprints201909.0185.v1

The overall reaction responsible for such precipitation could be written as:

$$6Cu^{2+} + 6H_2O + BH_4^- \rightarrow 2Cu_2O + 2Cu^0 + 12H^+ + B(OH)_4^- \quad \text{(Eq. 1)}$$

The subsequent SEM study carried out indicate that the solid is formed by nanoparticles agglomerates having various shapes: nanoplates and octahedral, characteristics of the Cu_2O/Cu phases nanostructures [32,33].

2.4. Adsorption mechanisms

Adsorption process mechanism can be controlled by a several diffusion steps: (a) film diffusion (bulk diffusion and external film diffusion; (b) particle diffusion (intraparticle or internal diffusion); (c) moving boundary process, proper sorption reaction between sorbent and active sites, mass action; apart of chemical reaction that may contribute to the control of mass transfer [34].

The calculated parameters for each of the different studied models [35] are summarized in Table 4. The obtained correlation coefficients show that the copper adsorption can be best explained by the moving boundary process.

Table 4. Kinetic constants of the different adsorption mechanism.

Model	R^2	k
film-diffusion	0.946	0.058
particle-diffusion	0.951	0.050
moving boundary	0.982	0.012

2.4. Statistical analysis

In order to know the influence of various variables, copper concentration (A), pH (B) and carbon dosage (C) in the adsorption of Cu(II) onto AC a full factorial design of 23 were done [36,37]. By means of the statistical analysis of the factor considered, the Pareto chart allows to detect the factor and interaction effects that are considered statically significant with a p-values <0.05 [38,39]. The only statically significant factor is the pH see Figure 7, the positive sign indicates a positive effect between an increase in the pH and the percentage of copper adsorbed.

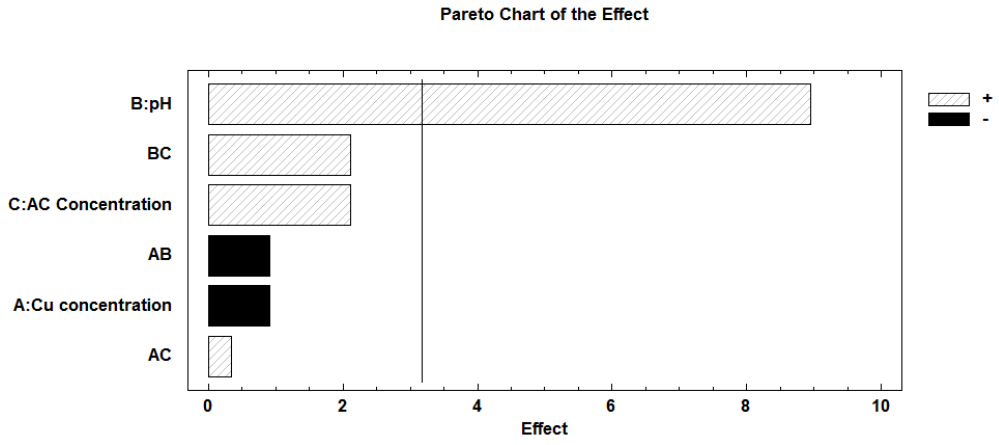

Figure 7. Pareto chart diagram.

The mathematical model obtained for this design was:

Preprints (www.preprints.org) | NOT PEER-REVIEWED | Posted: 17 September 2019 doi:10.20944/preprints201909.0185.v1

$$\text{Elimination (\%)} = 37.52 - 3.553\cdot[\text{Cu(II)}] + 34.595\cdot\text{pH} + 8.183\cdot[\text{AC}] - 3.553\cdot[\text{Cu(II)}]\cdot\text{pH} + 1.33\cdot[\text{Cu(II)}]\cdot[\text{AC}] + 8.183\cdot\text{pH}\cdot[\text{AC}] \quad \text{(Eq. 2)}$$

where R^2 were 96.81.

Figure 8 shows the response surface as a function of two factor keeping the other factor at certain level, this is the best way to evaluate the relationship between the factor and response [40]. The graph a), shows an increases in Cu^{2+} adsorption with the increases of the pH, this rise looks like slightly higher for the lower copper concentration. In the case of pH and AC concentration, graph b), the behavior is similar an increases in the pH arise the copper removal percentage, this effect is more remarkable for the higher level of AC concentration.

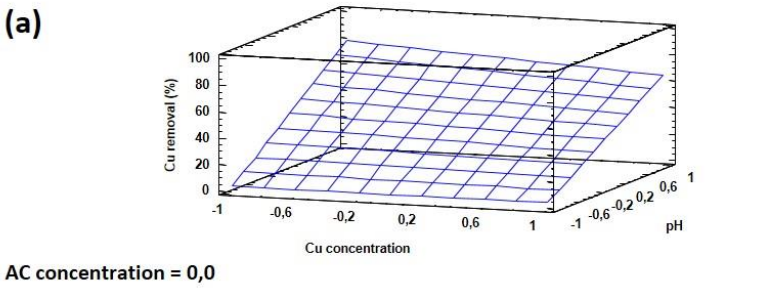

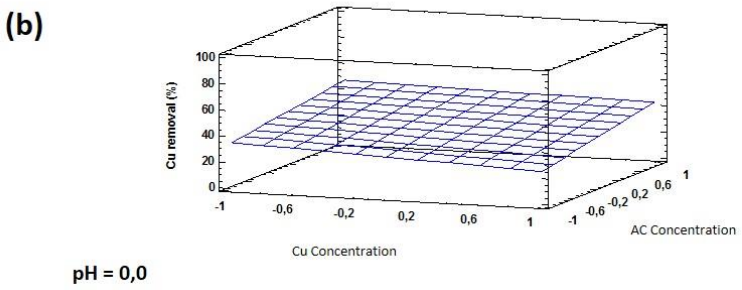

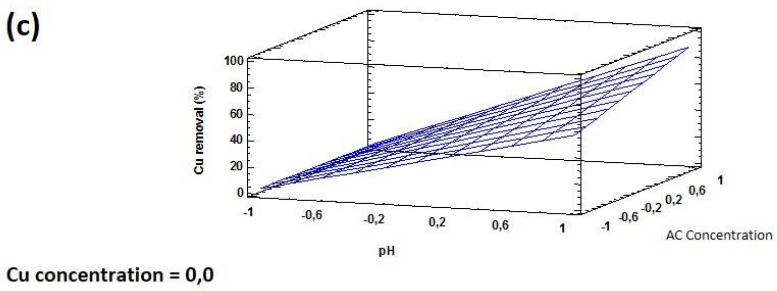

Figure 8. Response surface plot for cupper metal removal (%). a) Cu concentration-pH effect; b) pH-AC concentration; c) Cu concentration-AC concentration.

Preprints (www.preprints.org) | NOT PEER-REVIEWED | Posted: 17 September 2019 doi:10.20944/preprints201909.0185.v1

Figure 9 shows the cube graph to the copper removal percentage, the optimum recovery percentage of Cu(II) obtained with the model is 94.26% according to the conditions A: Cu Concentration of 5 mg·L-1, B: pH 5 and C: AC dosage 75 mg.

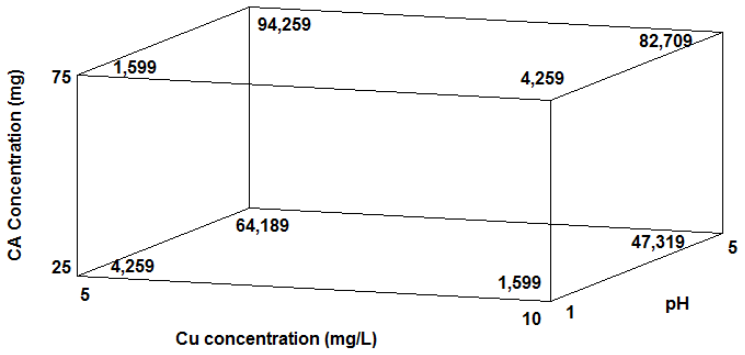

Figure 9. The cube graph of copper removal percentage.

3. Materials and Methods

3.1. Obtention of the activated carbon

Activated carbon (AC) from a winemaking waste, bagasse, were obtained as described [10,18]: an aqueous suspension of bagasse waste (75 g·L^{-1}) of the production of Albariño wine (Denomination of Origin 'Rías Baixas', Galicia) and supplied by the Misión Biológica de Galicia (CSIC), was introduced into a Berghof BR300 high pressure reactor at 523 K and 30 bars for 3 h. The obtained mixture was filtered to separate the generated hydrothermal carbon (HTC), which was dried. A mixture HTC/KOH (weight ratio 1:2) was introduced at 1073 K for 2 h in a Carbolite STF 15 tubular furnace under a N_2 atmosphere (150 mL·min^{-1}) in order to generated the AC. After cooling down to room temperature, the AC was washed with MilliQ water until pH~5. Finally, the AC was dried at 353 K.

3.2. Characterization of the activated carbon

Zeta potential measurements were carried out using a Zetasizer Malvern Nano ZS (Malvern Panalytical Ltd., Worcestershire, UK) at 298 K. Aqueous suspensions were prepared between the pH range of 1 and 7 using HCl 0.1 M. All solutions were dispersed with a sonicator Bandelin Electronic Sonopuls HD 3100, (Bandelin electronic GmbH & Co. KG, Berlin, Germany) with amplitude of 80% for 300 s.

The porous structure of the activated carbon was characterized by N_2 adsorption at 77 K using the Micromeritics ASAP, 2020 Accelerated Surface Area and Porosimetry System. The sample was partially degassed at 623 K for 16 h. The specific surface was determined by analyzing the adsorption isotherm via the BET equation and DFT models, employing Micromeritics and Quantachrome software. The obtained results exhibit that the microporous surface (S_{mi}) of the AC was 1111 m^2·g^{-1} and the S_{BET} 2662 m^2·g^{-1}. In addition, the size of the pores were <2 nm (Average micropore size, L_o = 1.71). So, the AC show a microporous structure indicating that the material is suitable for metal adsorption.

3.3. Batch adsorption experiments

The metal adsorption by the activated carbon was carried out via batch experiments performed in Erlenmeyer flasks. The control of the temperature was performed using a Selecta Termotronic thermostat-controlled bath equipped with multiple Lab Companion MS-52M stirrers until equilibrium was reached. The stirring speed was constant for all adsorption experiment at 500

Preprints (www.preprints.org) | NOT PEER-REVIEWED | Posted: 17 September 2019 doi:10.20944/preprints201909.0185.v1

revolutions per minute (rpm). 1 mL of sample were collected at 0, 5, 10, 20, 30, 40, 50, 60, 120 and 180 min and filtered through a syringe filters with a 0.22 μm pore and 13 mm diameter.

Copper content in the solution was analyzed by AAS spectrometry and the copper content in the carbon was estimated by the mass balance. The pH of the solutions was adjusted using a pH meter and adding HCl (0.1 M). The adsorption capacity (q_e (mg·g^{-1})) was calculated by following equations:

$$q_e = \frac{(C_0 - C_e)\cdot V}{m} \quad \text{(Eq. 3)}$$

where C_0 (mg·L^{-1}) is the initial concentration of copper in solution, C_e (mg·L^{-1}) is the copper concentration at equilibrium, q_e (mg·g^{-1}) is the amount of copper adsorbed on the activated carbon at equilibrium, V (L) is the volume of the solution and m (g) is the mass of the activated carbon.

The equilibrium adsorption isotherm data were plotted using the Langmuir, Freundlich and Temkin linear forms models [41]:

$$\text{Langmuir:} \quad \frac{C_e}{q_e} = \frac{1}{q_m \cdot b} + \frac{1}{q_m}\cdot c_e \quad \text{(Eq. 4)}$$

$$\text{Freundlich:} \quad \ln q_e = \ln K_F + \frac{1}{n}\cdot \ln C_e \quad \text{(Eq. 5)}$$

$$\text{Temkin:} \quad q_e = B \cdot \ln A_T + B \cdot \ln c_e \quad \text{(Eq. 6)}$$

where q_e (mg·g^{-1}) is adsorbed metal amount by mass of activated carbon in the equilibrium; K_F (L·g^{-1}) is the Freundlich constant; 1/n is indicative of the intensity of adsorption; qm (mg·g^{-1}) is the maximum adsorption capacity of the adsorbent per unit mass of adsorbate; b (L·mg^{-1}) is the Langmuir constant related with the adsorption energy; C_e (mg·L^{-1}) is the metal concentration in the equilibrium; A_T Temkin isotherm equilibrium binding constant (L·g^{-1}); B (R·T/b_T) constant related to heat of sorption (J·mol^{-1}); b_T Temkin isotherm constant; R universal gas constant (8.314·103 kJ·K^{-1}·mol^{-1}) and R_L is the adimensional Langmuir constant or the equilibrium parameter and indicates if the isotherm is reversible (R_L=0), favorable (0<R_L<1), lineal (R_L=1) or unfavorable (R_L>1) where R_L=1/(1+b·Co).

The Batch kinetics experiments for copper adsorption on AC were carried out at different temperatures and were analyzed using the pseudo-first and pseudo-second order kinetics models:

pseudo-first order: $\ln(q_e - q_t) = \ln q_e - K_1 \cdot t$ (Eq. 7) [42]

pseudo-second order: $\frac{t}{q_t} = \frac{1}{K_2 \cdot q_e^2} + \frac{1}{q_e}\cdot t$ (Eq. 8) [43]

where q_t (mg·g^{-1}) is the adsorbed metal amount per mass of the activated carbon at different contact time (t) and at equilibrium qe (mg·g^{-1}); K_1 (L·min^{-1}) and K_2 (g·min·mg^{-1}) are the first and second order adsorption constant, respectively.

Thermal parameters were calculated from (Eq. 9) and (Eq. 10). Enthalpy change (ΔH^0) and entropy change (ΔS^0) were calculated from slope and intercept of a plot of log (q_e/c_e) versus 1/T according (Eq. 9) [44]:

$$\log \frac{q_e}{c_e} = \frac{\Delta S^0}{2.303R} + \frac{\Delta H^0}{2.303RT} \quad \text{(Eq. 9)}$$

$$\Delta G^0 = \Delta H^0 - T\Delta S^0 \quad \text{(Eq. 10)}$$

where R is the universal gas constant (8.314 J·mol^{-1}·K^{-1}); T the absolute temperature (K).

 doi:10.20944/preprints201909.0185.v1

The rate law that govern the copper adsorption by the activated carbon were assessed. Three possible adsorption mechanisms have been evaluated: the diffusion of Cu species from the aqueous solution to the AC surface (Eq. 11) [45], the diffusion of ions within the AC (Eq. 12) [46] and the moving boundary process (Eq. 13) [47]:

film-diffusion controlled mechanism: $ln(1-F) = -k \cdot t$ (Eq. 11)

particle-diffusion controlled mechanism: $ln(1-F^2) = -k \cdot t$ (Eq. 12)

moving boundary mechanism: $3 - 3 \cdot (1-F)^{\frac{2}{3}} - 2 \cdot F = k \cdot t$ (Eq. 13)

where k is the corresponding constant and F is defined to (Eq. 14):

$$F = \frac{[AM]_t}{[AM]_e} \quad \text{(Eq. 14)}$$

where $[AM]_t$ and $[AM]_e$ are the concentrations of metal adsorbed after a time (t) and in equilibrium (e), respectively.

The surface of the AC and the AC loaded with Cu (AC-Cu) was examined by field emission scanning electron microscope (FE-SEM) using a JEOL JSM 7600 microscope and X-ray photoelectron spectroscopy (XPS). Spectra were recorded using a Fisons MT500 spectrometer equipped with a hemispherical electron analyzer (CLAM2) and a non-monochromatic Mg K_α X-Ray source operated at 300 W. Spectra were collected at a pass energy of 20 eV (typical for high-resolution conditions). The area under each peak was calculated after subtraction of the S-shaped background and fitting the experimental curve to a combination of Lorentzian and Gaussian lines of variable proportions. Binding energies were calibrated to the C 1s peak at 285.0 eV. The atomic ratios were computed from the peak intensity ratios and reported atomic sensitivity factors.

The structural characterization was carried out through X-ray diffraction (XRD) using a Siemens D5000 diffractometer equipped with a Cu anode (Cu K_α radiation) and a LiF monochromator.

3.4. Experimental design

In order to estimate the major effect and higher-order interaction a full factorial 2k design was used. Three parameters and two levels for each parameter were analyzed 23. Where the three factors pH, metal concentration and AC amount were selected as independent variables and the response variable was the Cu(II) removal percentage. The independent variables were varied at two levels, upper and lower limits for each one. Area total of 10 experiments were carried out 2^3=8 and 2 central point. The experiments were done at 500 rpm and room temperature. The design of experiment was constructed and analyzed using Statgraphics centrurion XVI version, 13.2.04. The significant factor where studied according to Pareto charts and analysis of variance (ANOVA) testing at 95% confidence.

4. Conclusions

Activated carbon from winemaking wastes was used to copper removed in aqueous solutions. In addition, competitive adsorption with other metal was also investigated. Different parameters which affect to the metal adsorption were assessed. Kinetic studies show that the Cu adsorption is better adjusted to a second-order kinetic. The experimental results fit a Langmuir isotherm. Thermodynamic studies have shown that the copper adsorption is an exothermic, spontaneous and favorable process. Also, the law that govern the adsorption was the moving boundary process. In addition, it is possible the recovery of zero valent copper from the eluates, thought this step must be investigated more deeply. The full factorial experimental design showed that the pH and the pH-AC dosage interaction have a great effect in the Cu removed process. The optimal conditions obtained by the design of the experiments was 5 $mg \cdot L^{-1}$ Cu concentration, pH 5 and 10 mg AC dosage.

Therefore, the active carbon obtained from winemaking wastes is useful for Cu^{2+} removal from wastewater.

Author Contributions: For research articles with several authors, a short paragraph specifying their individual contributions must be provided. The following statements should be used "conceptualization, F.J.A. and F.A.L.; methodology, L.A. and F.A.L.; validation, F.J.A. and F.A.L. formal analysis, I.G.-D.; investigation, L.A., F.A.L. and F.J.A.; resources, F.A.L.; writing—original draft preparation, L.A. and F.J.A.; writing—review and editing, L.A. and F.A.L.

Funding: "This research was funded by ESTANNIO Programme, grant number RTC-2017-6629-5 (Spanish Ministry of Science, Innovation and Universities". We acknowledge support of the publication fee by the CSIC Open Access Publication Support. Initiative through its Unit of Information Resources for Research (URICI).

Acknowledgments: The authors would like the Dr. Irene Llorente (CENIM-CSIC) for performing the XPS measurements.

Conflicts of Interest: The authors declare no conflict of interest.

References

1. Demiral, H.; Güngör, C. Adsorption of copper(II) from aqueous solutions on activated carbon prepared from grape bagasse. *J. Clean. Prod.* **2016**, *124*, 103–113.
2. Aydın, H.; Bulut, Y.; Yerlikaya, Ç. Removal of copper (II) from aqueous solution by adsorption onto low-cost adsorbents. *J. Environ. Manage.* **2008**, *87*, 37–45.
3. Feng, N.; Guo, X.; Liang, S. Adsorption study of copper (II) by chemically modified orange peel. *J. Hazard. Mater.* **2009**, *164*, 1286–1292.
4. Sudha Rani, K.; Srinivas, B.; Gourunaidu, K.; Ramesh, K. V. Removal of copper by adsorption on treated laterite. *Mater. Today Proc.* **2018**, *5*, 463–469.
5. Ferreira da Silva, A.J.; Paiva de Alencar Moura, M.C.; da Silva Santos, E.; Saraiva Pereira, J.E.; Lins de Barros Neto, E. Copper removal using carnauba straw powder: Equilibrium, kinetics, and thermodynamic studies. *J. Environ. Chem. Eng.* **2018**, *6*, 6828–6835.
6. Coudert, L.; Blais, J.-F.; Mercier, G.; Cooper, P.; Gastonguay, L.; Morris, P.; Janin, A.; Reynier, N. Pilot-scale investigation of the robustness and efficiency of a copper-based treated wood wastes recycling process. *J. Hazard. Mater.* **2013**, *261*, 277–285.
7. Ntimbani, R.N.; Simate, G.S.; Ndlovu, S. Removal of copper ions from dilute synthetic solution using staple ion exchange fibres: Equilibrium and kinetic studies. *J. Environ. Chem. Eng.* **2015**, *3*, 1258–1266.
8. Kalaiselvi, G.; Maheswari, P.; Mohan, D.; Balasubramanian, S. Synthesis and characterization of poly 3-methyl 2-vinyl pyridinium nitrate incorporated polyvinylidine fluoride ultrafiltration membrane for metal ion removal. *Sep. Purif. Technol.* **2015**, *143*, 105–114.
9. Carvalho Barros, G.K.G.; Melo, R.P.F.; Barros Neto, E.L. de Removal of copper ions using sodium hexadecanoate by ionic flocculation. *Sep. Purif. Technol.* **2018**, *200*, 294–299.
10. Alcaraz, L.; López Fernández, A.; García-Díaz, I.; López, F.A. Preparation and characterization of activated carbons from winemaking wastes and their adsorption of methylene blue. *Adsorpt. Sci. Technol.* **2018**, *36*, 1331–1351.
11. Hu, Z.; Srinivasan, M.. Preparation of high-surface-area activated carbons from coconut shell. *Microporous Mesoporous Mater.* **1999**, *27*, 11–18.

12. Liew, R.K.; Chai, C.; Yek, P.N.Y.; Phang, X.Y.; Chong, M.Y.; Nam, W.L.; Su, M.H.; Lam, W.H.; Ma, N.L.; Lam, S.S. Innovative production of highly porous carbon for industrial effluent remediation via microwave vacuum pyrolysis plus sodium-potassium hydroxide mixture activation. *J. Clean. Prod.* **2019**, *208*, 1436–1445.
13. Yek, P.N.Y.; Liew, R.K.; Osman, M.S.; Lee, C.L.; Chuah, J.H.; Park, Y.K.; Lam, S.S. Microwave steam activation, an innovative pyrolysis approach to convert waste palm shell into highly microporous activated carbon. *J. Environ. Manage.* **2019**, *236*, 245–253.
14. Pallarés, J.; González-Cencerrado, A.; Arauzo, I. Production and characterization of activated carbon from barley straw by physical activation with carbon dioxide and steam. *Biomass and Bioenergy* **2018**, *115*, 64–73.
15. Sajjadi, S.A.; Mohammadzadeh, A.; Tran, H.N.; Anastopoulos, I.; Dotto, G.L.; Lopičić, Z.R.; Sivamani, S.; Rahmani-Sani, A.; Ivanets, A.; Hosseini-Bandegharaei, A. Efficient mercury removal from wastewater by pistachio wood wastes-derived activated carbon prepared by chemical activation using a novel activating agent. *J. Environ. Manage.* **2018**, *223*, 1001–1009.
16. Duan, X. Preparation of High Surface Area Activated Carbon from Coconut Shells Using Microwave Heating. *Bioresour. Technol.* **2010**, *101*, 6163–6169.
17. Kaouah, F.; Boumaza, S.; Berrama, T.; Trari, M.; Bendjama, Z. Preparation and characterization of activated carbon from wild olive cores (oleaster) by H3PO4 for the removal of Basic Red 46. *J. Clean. Prod.* **2013**, *54*, 296–306.
18. Alguacil, F.J.; Alcaraz, L.; García-Díaz, I.; López, F.A. metals Removal of Pb 2+ in Wastewater via Adsorption onto an Activated Carbon Produced from Winemaking Waste. **2018**.
19. Burakov, A.E.; Galunin, E. V.; Burakova, I. V.; Kucherova, A.E.; Agarwal, S.; Tkachev, A.G.; Gupta, V.K. Adsorption of heavy metals on conventional and nanostructured materials for wastewater treatment purposes: A review. *Ecotoxicol. Environ. Saf.* **2018**, *148*, 702–712.
20. Madhavarao, M.; Ramesh, A.; Purnachandrarao, G.; Seshaiah, K. Removal of copper and cadmium from the aqueous solutions by activated carbon derived from Ceiba pentandra hulls. *J. Hazard. Mater.* **2006**, *129*, 123–129.
21. Al-Homaidan, A.A.; Al-Houri, H.J.; Al-Hazzani, A.A.; Elgaaly, G.; Moubayed, N.M.S. Biosorption of copper ions from aqueous solutions by Spirulina platensis biomass. *Arab. J. Chem.* **2014**, *7*, 57–62.
22. Deihimi, N.; Irannajad, M.; Rezai, B. Equilibrium and kinetic studies of ferricyanide adsorption from aqueous solution by activated red mud. *J. Environ. Manage.* **2018**, *227*, 277–285.
23. Boparai, H.K.; Joseph, M.; O'Carroll, D.M. Kinetics and thermodynamics of cadmium ion removal by adsorption onto nano zerovalent iron particles. *J. Hazard. Mater.* **2011**, *186*, 458–465.
24. Oh, J.-Y.; You, Y.-W.; Park, J.; Hong, J.-S.; Heo, I.; Lee, C.-H.; Suh, J.-K. Adsorption characteristics of benzene on resin-based activated carbon under humid conditions. *J. Ind. Eng. Chem.* **2018**.
25. Ko, T.J.; Her, E.K.; Shin, B.; Kim, H.Y.; Lee, K.R.; Hong, B.K.; Kim, S.H.; Oh, K.H.; Moon, M.W. Water condensation behavior on the surface of a network of superhydrophobic carbon fibers with high-aspect-ratio nanostructures. *Carbon N. Y.* **2012**, *50*, 5085–5092.
26. Farzana, R.; Rajarao, R.; Bhat, B.R.; Sahajwalla, V. Performance of an activated carbon supercapacitor electrode synthesised from waste Compact Discs (CDs). *J. Ind. Eng. Chem.* **2018**, *65*, 387–396.
27. Choong, C.E.; Lee, G.; Jang, M.; Park, C.M.; Ibrahim, S. One step hydrothermal synthesis of magnesium silicate impregnated palm shell waste activated carbon for copper ion removal. *Metals (Basel).* **2018**, *8*.
28. Li, B.; Luo, X.; Zhu, Y.; Wang, X. Immobilization of Cu(II) in KIT-6 supported Co_3O_4 and catalytic

performance for epoxidation of styrene. *Appl. Surf. Sci.* **2015**, *359*, 609–620.

29. Liu, L.; Li, W.; Xiong, Z.; Xia, D.; Yang, C.; Wang, W.; Sun, Y. Synergistic effect of iron and copper oxides on the formation of persistent chlorinated aromatics in iron ore sintering based on in situ XPS analysis. *J. Hazard. Mater.* **2018**.

30. Espinós, J.P.; Morales, J.; Barranco, A.; Caballero, A.; Holgado, J.P.; González-Elipe, A.R. Interface Effects for Cu, CuO, and Cu_2O Deposited on SiO_2 and ZrO_2 . XPS Determination of the Valence State of Copper in Cu/SiO_2 and Cu/ZrO_2 Catalysts. *J. Phys. Chem. B* **2002**, *106*, 6921–6929.

31. Chanquía, C.M.; Sapag, K.; Rodríguez-Castellón, E.; Herrero, E.R.; Eimer, G.A. Nature and Location of Copper Nanospecies in Mesoporous Molecular Sieves. *J. Phys. Chem. C* **2010**, *114*, 1481–1490.

32. Wei, W. Controllable Synthesis and Catalytic Property of Novel Copper Oxides (CuO and Cu₂O) Nanostructures. *Int. J. Mater. Sci. Appl.* **2016**, *5*, 18.

33. Won, Y.H.; Stanciu, L.A. Cu_2O and Au/Cu_2O particles: Surface properties and applications in glucose sensing. *Sensors (Switzerland)* **2012**, *12*, 13019–13033.

34. Krys, P.; Testa, F.; Trochimczuk, A.; Pin, C.; Taulemesse, J.M.; Vincent, T.; Guibal, E. Encapsulation of ammonium molybdophosphate and zirconium phosphate in alginate matrix for the sorption of rubidium(I). *J. Colloid Interface Sci.* **2013**, *409*, 141–150.

35. Qiu, H.; Zhang, Q.; Lv, L.; Pan, B.; Zhang, W.; Zhang, Q. Critical review in adsorption kinetic models. *J. Zhejiang Univ. A* **2009**, *10*, 716–724.

36. Ghaedi, A.M.; Panahimehr, M.; Nejad, A.R.S.; Hosseini, S.J.; Vafaei, A.; Baneshi, M.M. Factorial experimental design for the optimization of highly selective adsorption removal of lead and copper ions using metal organic framework MOF-2 (Cd). *J. Mol. Liq.* **2018**, *272*, 15–26.

37. Maneechakr, P.; Samerjit, J.; Uppakarnrod, S.; Karnjanakom, S. Experimental design and kinetic study of ultrasonic assisted transesterification of waste cooking oil over sulfonated carbon catalyst derived from cyclodextrin. *J. Ind. Eng. Chem.* **2015**, *32*, 128–136.

38. Saleh, T.A.; Adio, S.O.; Asif, M.; Dafalla, H. Statistical analysis of phenols adsorption on diethylenetriamine-modified activated carbon. *J. Clean. Prod.* **2018**, *182*, 960–968.

39. Adio, S.O.; Omar, M.H.; Asif, M.; Saleh, T.A. Arsenic and selenium removal from water using biosynthesized nanoscale zero-valent iron: A factorial design analysis. *Process Saf. Environ. Prot.* **2017**, *107*, 518–527.

40. Mourabet, M.; El Rhilassi, A.; El Boujaady, H.; Bennani-Ziatni, M.; El Hamri, R.; Taitai, A. Removal of fluoride from aqueous solution by adsorption on Apatitic tricalcium phosphate using Box–Behnken design and desirability function. *Appl. Surf. Sci.* **2012**, *258*, 4402–4410.

41. Aljeboree, A.M.; Alshirifi, A.N.; Alkaim, A.F. Kinetics and equilibrium study for the adsorption of textile dyes on coconut shell activated carbon. *Arab. J. Chem.* **2017**, *10*, S3381–S3393.

42. S. Lagergren Zur Theorie der sogenannten Adsorption gelöster Stoffe. *Handlingar* **1898**, *24*, 1–39.

43. Ho, Y..; McKay, G. Pseudo-second order model for sorption processes. *Process Biochem.* **1999**, *34*, 451–465.

44. Fouodjouo, M.; Fotouo-Nkaffo, H.; Laminsi, S.; Cassini, F.A.; de Brito-Benetoli, L.O.; Debacher, N.A. Adsorption of copper (II) onto cameroonian clay modified by non-thermal plasma: Characterization, chemical equilibrium and thermodynamic studies. *Appl. Clay Sci.* **2017**, *142*, 136–144.

45. Chiarizia, R.; Horwitz, E.P.; Alexandratos, S.D. Uptake of metal ions by a new chalating ion-exchange resin. Part 4: Kinetics. *Solvent Extr. Ion Exch.* **1994**, *12*, 211–237.

46. Saha, B.; Iglesias, M.; Dimming, I.W.; Streat, M. Sorption of trace heavy metals by thiol containing

 doi:10.20944/preprints201909.0185.v1

chelating resins. *Solvent Extr. Ion Exch.* **2000**, *18*, 133–167.

47. Chanda, M.; Rempel, G.L. Quaternized Poly(4-vinylpyridine) Gel-Coated on Silica.Fast Kinetics of Diffusion-Controlled Sorption of Organic Sulfonates. *Ind. Eng. Chem. Res.* **1994**, *33*, 623–630.

Sample Availability: Not available.